Turbulent Flow and Large Surface Wave Events in the Marine Boundary Layers

Peter P. Sullivan
National Center for Atmospheric Research
Boulder, CO 80307-3000
Phone:(303) 497-8953 fax:(303) 497-8171 email: pps@ucar.edu

James C. McWilliams
Department of Atmospheric Sciences and
Institute of Geophysics and Planetary Physics, UCLA
Los Angeles, CA 90095-1565
Phone:(310) 206-2829 fax:(310) 206-5219 email: jcm@atmos.ucla.edu

Grant Number: N00014-07-M-0516

LONG-TERM GOALS

The long term objective of our research for the "High Resolution Air-Sea Interaction" (HIRES) Departmental Research Initiative (DRI) is to identify the couplings between large wave events, winds, and currents in the surface layer of the marine boundary layers. Turbulence resolving large eddy simulations (LESs) and direct numerical simulations (DNSs) of the marine atmospheric boundary layer (MABL) in the presence of time and space varying wave fields will be the main tools used to elucidate wind-wave-current interactions. A suite of turbulence simulations over realistic seas using idealized and observed pressure gradients will be carried out to compliment the field observations collected in moderate to high winds. The database of simulations will be used to generate statistical moments, interrogated for coherent structures, and ultimately used to compare with HIRES observations.

OBJECTIVES

Our goals are: 1) participate in the planning process for the HIRES field campaign; and 2) construct and exercise an LES code applicable to the HIRES high wind regime.

APPROACH

We are investigating interactions between the MABL and the connecting air-sea interface primarily using LES. The waves are externally imposed based on well established empirical wave spectra. Ultimately they will be provided by direct observations of the sea surface from the HIRES field campaign. The main technical advance is the development of a computational tool that allows for nearly arbitrary 3-D wave fields, *i.e.,* the sea surface elevation $h = h(x, y, t)$ as a surface boundary condition. The computational method allows for time and space varying surface conditions over a range of wave scales $\mathcal{O}(10)$m or larger as shown below.

Report Documentation Page

Form Approved
OMB No. 0704-0188

1. REPORT DATE	2. REPORT TYPE	3. DATES COVERED
30 SEP 2012		**00-00-2012 to 00-00-2012**

4. TITLE AND SUBTITLE	5a. CONTRACT NUMBER
Turbulent Flow and Large Surface Wave Events in the Marine Boundary Layers	5b. GRANT NUMBER
	5c. PROGRAM ELEMENT NUMBER
6. AUTHOR(S)	5d. PROJECT NUMBER
	5e. TASK NUMBER
	5f. WORK UNIT NUMBER
7. PERFORMING ORGANIZATION NAME(S) AND ADDRESS(ES) **National Center for Atmospheric Research,Boulder,CO,80307-3000**	8. PERFORMING ORGANIZATION REPORT NUMBER
9. SPONSORING/MONITORING AGENCY NAME(S) AND ADDRESS(ES)	10. SPONSOR/MONITOR'S ACRONYM(S)
	11. SPONSOR/MONITOR'S REPORT NUMBER(S)

12. DISTRIBUTION/AVAILABILITY STATEMENT
Approved for public release; distribution unlimited

13. SUPPLEMENTARY NOTES

14. ABSTRACT

15. SUBJECT TERMS

16. SECURITY CLASSIFICATION OF:			17. LIMITATION OF ABSTRACT	18. NUMBER OF PAGES	19a. NAME OF RESPONSIBLE PERSON
a. REPORT **unclassified**	b. ABSTRACT **unclassified**	c. THIS PAGE **unclassified**	**Same as Report (SAR)**	**11**	

WORK COMPLETED

Meetings: We attended the *Ocean Sciences Meeting* in Salt Lake City, UT and the *20th Symposium on Boundary Layers and Turbulence* joint with the *18th Conference on Air-Sea Interaction* in Boston, MA where we presented results from research funded by HIRES and the companion DRI Impact of Typhoons on the Ocean in the Pacific (ITOP). During the past year, we also collaborated extensively with numerous investigators who also presented results from current research at these meetings. The research spanned a broad range of topics in the atmospheric and oceanic boundary layers. A summary of the presentation titles and archival manuscripts produced during the past year are given in the PUBLICATIONS section of this report. We also participated in the HIRES PI meeting at Scripps Institution of Oceanography held in April 2012.

Table 1: Simulation properties

Run	U_g (m s^{-1})	$\mathcal{A} = C_p/U_{10}$	u_* (m s^{-1})	Q_* (K m s^{-1})	L
A	5	4.8	0.124	0.0	∞
AC	5	4.8	0.166	0.01	-35.0
ACF	5	–	0.167	0.01	-35.6
B	7.5	3.4	0.187	0.0	∞
C	10	2.8	0.228	0.0	∞
D	15	1.9	0.338	0.0	∞
E	20	1.5	0.452	0.0	∞
EB	20	–	0.471	0.0	∞
EC	20	1.5	0.539	0.01	-1200.0

Simulations: During the course of the HIRES DRI, we built a database of LES solutions that examine the influence of wave age on MABLs driven by a combination of shear and convective forcing. Often the wind driven MABL is either cooled or heated at the surface and thus it is of interest to consider flow over waves in the presence of atmospheric stability. Previously, we examined the impact of stratification using DNS (Sullivan & McWilliams, 2002) and LES (Sullivan *et al.*, 2008) over an idealized monochromatic wave. Table 1 lists bulk properties of the simulations, *viz.,* the geostrophic wind U_g, wave age $\mathcal{A} = C_p/U_{10}$, friction velocity u_*, surface heat flux Q_*, and Monin-Obukhov stability index L. In the definition of wave age, C_p denotes the phase speed of the peak in the wave height spectrum (see description below) and U_{10} is the reference wind speed at a height of 10 m above the water surface. The height of the MABL in these simulations is $z_i \sim 500$ m and in the experiments with unstable surface forcing the Deardorff (1972) convective scale $w_* \sim 0.53$ m s^{-1}. Simulations (without wave effects) are in a mixed shear-convective regime that tend to develop broad streamwise rolls (*e.g.,* Moeng & Sullivan, 1994). In addition to the simulations with a wavy lower boundary we also consider a run ACF with a flat lower boundary as a reference for run AC and a run EB with a stationary lower wavy surface (or bumps) for comparison with run E. In all the LES experiments, the computational domain is $(X_L, Y_L, Z_L) = (1200, 1200, 800)$ m and is discretized using $(N_x, N_y, N_z) = (512, 512, 128)$ gridpoints. A description of the code and first results are described in Sullivan *et al.*(2010a). We note that the algorithmic formulation is general and also allows turbulence simu-

lations over and around 3D stationary orography as described in Sullivan *et al.*(2010b) [1].

A broadband wave spectrum is considered in the numerical experiments with a wavy lower surface. The virtual surface wave field is built to match a wind-wave equilibrium Pierson and Moskowitz (1964) spectrum assuming a surface wind speed of 15 m s^{-1}; hence the phase speed of the peak in the wave spectrum $C_p \sim 18$ m s^{-1}. The individual wave modes in the wave spectrum are assumed to have random phases and a directional spectrum is picked to emphasize long crested waves. Each wave mode, resolved by the LES mesh, is advanced forward in time using the linear deep water dispersion relation. At each stage of the Runge-Kutta time stepping scheme we construct a new grid in physical space that fits the wavy surface. At a particular (x, y) gridpoint the stretched vertical grid spans $h(x, y, t) \leq z \leq Z_L$ where $h(x, y, t)$ is the instantaneous wave height and Z_L is a fixed height above the water surface (independent of (x, y, t)). An $x - y$ view of the 3D surface wave field at a particular instant in time is given in figure 1 and an oblique cutout view of the computational grid above the waves is depicted in figure 2. Additional details of the LES experimental design are provided in prior year progress reports.

RESULTS

In previous reports, we described the impact of surface waves on low-order statistical moments, *viz.,* mean winds, vertical momentum fluxes, and turbulence variances (*e.g.,* see figures 3 and 4). In order to link statistics with flow events and structures we carried out extensive flow visualization and constructed animations of select flow variables from the database of available LES solutions summarized in Table 1. An interesting (typical) result is presented in the three panel plot of figure 5 where we compare the instantaneous static pressure $\overline{p}'/\rho$ and flow vectors $(\overline{u} - u_c, \overline{w})$ for simulations EB, E, and A. Following Adrian *et al.* (2000) we choose the constant velocity u_c so as to expose the rotational (vortical) motions in the surface layer. In each simulation the surface boundary conditions imposed at the bottom boundary of the LES are identical, *viz.,* the resolved wave spectrum and the small scale surface roughness z_o. All three simulations are performed with neutral stratification ($Q_* = 0$ at the surface) but with varying geostrophic winds (see Table 1).

Inspection of the flow fields presented in the $x - z$ vertical slices of figure 5 clearly shows the impact of surface waves on the turbulent surface layer winds for varying wave age. For the stationary bump case EB (no moving waves) we observe that the pressure field is strongly correlated with the underlying wave shape, *i.e.,* (negative, positive) $\overline{p}'/\rho$ is well correlated with wave (crests, troughs), respectively, with coherent pressure signals extending upwards to 20 m or more. This is the expected pattern for turbulent flow over low amplitude hills in the absence of flow separation (*e.g.,* Gong *et al.* 1996). The middle panel is a typical flow pattern that occurs with moving surface waves when the wave age is near equilibrium $\mathcal{A} \sim 1.5$. In this situation the pressure field induced by the surface waves is dramatically weaker than in the stationary bump case and there is only a faint correlation between $\overline{p}'/\rho$ and the wave shape $h(x, y)$. Essentially, most of the long wavelength (resolved) surface waves are traveling near the local wind speed and as a result these long waves induce only small perturbations in the surface winds. The absence of a significant pressure-wave slope correlation implies that the form drag induced by long wavelength waves $\lambda > \mathcal{O}(10\,\mathrm{m})$ in these simulations is small. In other words, when winds and waves are near equilibrium $\mathcal{A} \sim 1.2$ the bulk of the form stress (drag) is supported by slowly

[1] The meeting papers Sullivan *et al.*, (2010a,b) are available at http://www.mmm.ucar.edu/people/sullivan/.

propagating small scale waves (*e.g.,* Makin *et al.* 1995). The surface-elevated contours of negative pressure surrounded by spanwise rotating velocity vectors suggests that the dominant coherent structures in the wind-wave equilibrium boundary layer are likely hairpin vortices (*e.g.,* Adrian *et al.* 2000 and see discussion below). In the bottom panel of figure 5, a strong correlation between the pressure field and the underlying wave shape re-appears for wave age $\mathcal{A} \sim 4.8$; (negative, positive) $\overline{p}'/\rho$ is now well correlated with wave (crests, troughs), respectively. Animations clearly show these pressure patterns are connected to the motion of the surface waves as they propagate faster than the overlying winds. Wind-aligned swell (as depicted in figure 5) can be dynamically important as it generates a surface pressure field that reverses the sign of the form stress. Similar to Sullivan *et al.* (2008), on average the pressure pattern induced by our multi-mode fast propagating swell tilts slightly forward of the wave crests (*i.e.,* into the wind) resulting in positive form stress. This is an indication of "wave pumping" which can lead to a wave driven wind in the neutral boundary layer. Wave pumping combined with small amounts of convection can further modify Monin-Obukhov surface layer scaling and the bulk boundary layer properties (see figure 4 and Nilsson *et al.* 2012).

The neutral low-wind swell dominated case, with a broadband wave spectrum, is a particularly intriguing regime with the flow dynamics determined by the competing effects of airflow turbulence and wave pumping; the former tends to destroy the organization induced by the latter. A vast body of literature (*e.g.,* Zhou *et al.* 1999; Adrian *et al.* 2000; Christensen & Adrian, 2001) shows that in shear generated flat wall boundary layers the dominant coherent structures are packets of hairpin vortices. These vortices, which are found using various eduction schemes, critically impact the flow dynamics in both the lower and upper regions of flat wall boundary layers. We follow Adrian *et al.* (2001) and adopt the so-called λ_{ci} vortex detection method to identify the coherent structures in the low-wind swell dominated MABL. Mathematically λ_{ci} is the magnitude of the complex eigenvalue of the velocity gradient tensor $\partial u_i/\partial x_j$ and physically λ_{ci} is a measure of local swirling strength. In our simulations where a coordinate transformation is used to map physical space onto flat computational space the eigenvalues of the velocity gradient tensor are computed from the expression

$$\frac{\partial \overline{u}_i}{\partial x_j} = \frac{\partial \overline{u}_i}{\partial \xi_k}\frac{\partial \xi_k}{\partial x_j} \tag{1}$$

where $\partial \xi_k/\partial x_j$ are the metric components connecting physical and computational coordinates. The real and complex eigenvalues are found by solving the cubic characteristic equation implied by (1).

Figure 6 shows contours of λ_{ci} with an overlay of flow vectors for simulation A. The dark red colors are regions where the local swirling strength is particularly high. Also notice these regions are surrounded by spanwise rotating velocity vectors which adds confidence to our interpretation that high values of λ_{ci} are indeed vortical cores. Closer inspection of figure 6 shows that the dominate vortical motions rotate in a clockwise sense, are packed near the wavy surface, and are primarily found in the local wave troughs, *i.e.,* between wave crests. Animations further show the persistent character of this coherent structure and its forward propagation with the waves. This near surface vortical structure is distinctly different than the hairpin vortex packets typical of flat wall shear boundary layers and further emphasizes that MABLs can have unique dynamics depending on wave age.

IMPACT/APPLICATIONS

The computational tools developed and the database of numerical solutions generated will aide in the interpretation of the observations gathered during the past HIRES field campaign. In addition idealized process studies performed with the simulations have the potential to improve our understanding of the mechanisms that lead to surface drag under high wind conditions.

TRANSITIONS & RELATED PROJECTS

The current work is a collaborative effort between NCAR, university investigators and international research laboratories. Also the present work has links to the ONR DRI Impact of Typhoons on the Ocean in the Pacific (ITOP).

REFERENCES

Adrian, R. J., C. D. Meinhart & C. D. Tomkins, 2000: Vortex organization in the outer region of the turbulent boundary layer. *Journal of Fluid Mechanics*, **422**, 1–54.

Christensen, K. T. & R. J. Adrian, 2001: Statistical evidence of hairpin vortex packets in wall turbulence. *Journal of Fluid Mechanics*, **431**, 433-443.

Deardorff, J. W., 1972: Numerical investigation of neutral and unstable planetary boundary layers. *Journal of the Atmospheric Sciences*, **29**, 91-115.

Gong, W., P. A. Taylor & A. Dörnbrack, 1996: Turbulent boundary-layer flow over fixed aerodynamically rough two-dimensional sinusoidal waves. *Journal of Fluid Mechanics*, **312**, 1-37.

Makin, V. K., V. N. Kudryavtsev & C. Mastenbroek, 1995: Drag of the sea surface. Boundary-Layer Meteorology, **73**, 159-182.

Moeng, C.-H. & P. P. Sullivan, 1994: A comparison of shear and buoyancy driven planetary-boundary-layer flows. *Journal of the Atmospheric Sciences*, **51**, 999-1022.

Nilsson, E. O., A. Rutgersson & P. P. Sullivan, 2012: Convective boundary layer structure in the presence of wind-following swell. *Quarterly Journal of the Royal Meteorological Society*, [in press].

Sullivan, P. P. & J. C. McWilliams, 2002: Turbulent flow over water waves in the presence of stratification. *Physics of Fluids*, **14**, 1182-1195.

Sullivan, P. P., J. B. Edson, T. Hristov, & J. C. McWilliams, 2008: Large eddy simulations and observations of atmospheric marine boundary layers above non-equilibrium surface waves. *Journal of the Atmospheric Sciences*, **65**, 1225-1245.

Sullivan, P.P., 2010a: Large eddy simulation of high wind marine boundary layers above a spectrum of resolved moving waves. *19th Symposium on Boundary Layers and Turbulence*, Keystone, CO.

Sullivan, P.P., E. G. Patton & K. W. Ayotte, 2010b: Turbulent flow over and around sinusoidal bumps, hills, gaps and craters derived from large eddy simulations. *19th Symposium on Boundary Layers and Turbulence*, Keystone, CO.

Zhou, J., R. J. Adrian, S. Balachandar & T. M. Kendall, 1999: Mechanisms for gnerating coherent packets of hairpin vortices in channel flow, *Journal of Fluid Mechanics*, **387**, 353-396.

PUBLICATIONS

Sullivan, P. P., L. Romero, J. C. McWilliams & W. K. Melville, 2012: Transient evolution of Langmuir turbulence in ocean boundary layers driven by hurricane winds and waves. *Journal of Physical Oceanography*, [in press].

McWilliams, J. C., E. Huckle, J.-H. Liang & P. P. Sullivan, 2012: The wavy Ekman layer: Langmuir circulations, breakers, and Reynolds stress. *Journal of Physical Oceanography*, [in press].

Richter, D. H. & P. P. Sullivan, 2012: Momentum transfer in a turbulent, particle-laden Couette flow. *Physics of Fluids*, [submitted].

Suzuki, N., T. Hara & P. P. Sullivan, 2012: Impact of wave breaking wave form drag on near surface turbulence and drag coefficient over young seas at high winds. *Journal of Physical Oceanography*, [submitted].

Waggy, S. Biringen, & P. P. Sullivan, 2012: Direct simulation of top-down and bottom-up diffusion in the unstable Ekman layer. *Journal of Fluid Mechanics*, [submitted].

Belcher, S. E., A. A. L. M. Grant, K. E. Hanley, B. Fox-Kemper, L. Van Roekel, P. P. Sullivan, W. G. Large, A. Brown, A. Hines, D. Calvert, A. Rutgersson, H. Pettersson, J.-R. Bidlot, P. A. E. M. Janssen & J. A. Polton, 2012: A global perspective on Langmuir turbulence in the ocean surface boundary layer. *Geophysical Research Letters*, [accepted].

Weil, J. C., P.P. Sullivan, E. G. Patton & C-H. Moeng, 2012: Statistical variability of dispersion in the convective boundary layer: LPDM-LES model ensembles and observations. *Boundary-Layer Meteorology*, [in press].

Nilsson, E. O., A. Rutgersson & P. P. Sullivan, 2012: Convective boundary layer structure in the presence of wind-following swell. *Quarterly Journal of the Royal Meteorological Society*, [in press].

Van Roekel, L. P., B. Fox-Kemper, P. P. Sullivan, P. E. Hamlington, & S. R. Haney, 2012: The form and orientation of Langmuir cells for misaligned winds and waves. *Journal of Geophysical Research*, **117**, C05001.

Liang, J-H., J. C. McWilliams, P. P. Sullivan & B. Baschek, 2012: Large eddy simulation of the bubbly ocean: New insights on subsurface bubble distribution and bubble-mediated gas transfer. *Journal of Geophysical Research - Oceans*, **117**, C04002.

Kang, S.-L., D. H. Lenschow & P. P. Sullivan, 2012: Effects of mesoscale surface thermal heterogeneity on low-level horizontal wind speeds. *Boundary-Layer Meteorology*, **143**, 409-432.

Lenschow, D. H., M. Lothon, S. D. Mayor, P. P. Sullivan, & G. Canut, 2012: A comparison of higher-order vertical velocity moments in the convective boundary layer from lidar with in situ measurements and LES. *Boundary-Layer Meteorology*, **143**, 107-123.

Sullivan, P. P. & E. G. Patton, 2011: The effect of mesh resolution on convective boundary layer statistics and structures generated by large-eddy simulation. *Journal of the Atmospheric Sciences*, **68**, 2395-2415.

Hanley, K. E., S. E. Belcher & P. P. Sullivan, 2011: Response to "Comments on a global climatology of wind-wave interaction". *Journal of Physical Oceanography*, **41**, 1814-1817.

Moeng, C.-H. and P.P. Sullivan 2011: Large Eddy Simulation. Encyclopedia of Atmospheric Sciences 2nd Edition, Eds. G. North, F. Zhang and J. Pyle. Academic Press, [submitted].

Sullivan, P. P., T. Hristov & E. G. Patton, 2012: Marine atmospheric turbulence coupled to time-varying three-dimensional surface water waves: Results from LES. *20th Symposium on Boundary Layers and Turbulence*, Boston, MA.

Richter, D. & P. P. Sullivan, 2012: Turbulence modification in the presence of sea spray. *18th Conference on Air-Sea Interaction* Boston, MA.

Nguyen, K. X., S. P. Oncley, T. W. Horst, P. P. Sullivan, & C. Tong, 2012: Measurements of the budget of the subgrid-scale stress in convective atmospheric surface layers. *20th Symposium on Boundary Layers and Turbulence*, Boston, MA.

Nilsson, E., A. Rutgersson, E. Sahlé, A. Smedman & P. P. Sullivan, 2012: Influences of surface gravity waves on atmospheric boundary layer structure and fluxes. *20th Symposium on Boundary Layers and Turbulence*, Boston, MA.

Sullivan, P. P., L. Romero, W. K. Melville & J. C. McWilliams, 2012: Signatures of Langmuir turbulence in the hurricane OBL. *Ocean Sciences Meeting*, Salt Lake City, UT.

Liang, J-H., J. C. McWilliams, P. P. Sullivan & B. Baschek, 2012: Subsurface bubble distribution and its implication for boundary layer turbulence and air-sea gas transfer. *Ocean Sciences Meeting*, Salt Lake City, UT.

Richter, D. & P. Sullivan, 2012: Sea spray dynamics in the marine boundary layer. *Ocean Sciences Meeting*, Salt Lake City, UT.

Fox-Kemper, B., P. E. Hamlington, L. Van Roekel & P.P. Sullivan, 2012: Parameterization of submesoscale and Langmuir-scale processes and interactions. *Ocean Sciences Meeting*, Salt Lake City, UT.

Hamlington, P.E., L. Van Roekel, P.P. Sullivan, & B. Fox-Kemper 2012: Langmuir-submesoscale interactions: Multiscale simulations with the Craik-Leibovich squations. *Ocean Sciences Meeting*, Salt Lake City, UT.

Suzuki, N., T. Hara & P.P. Sullivan, 2012: Impacts of breaking waves on airflow at high wind conditions. *Ocean Sciences Meeting*, Salt Lake City, UT.

Kukulka, T., A. J. Plueddemann, J. H. Trowbridge, and P. P. Sullivan, 2012: The influence of crosswind tidal currents on Langmuir circulation in a shallow ocean. *Ocean Sciences Meeting*, Salt Lake City, UT.

Belcher, S. E., A. A. L. M. Grant, K. E. Hanley, B. Fox-Kemper, L. Van Roekel, P. P. Sullivan, W. G. Large, A. Brown, A. Hines, D. Calvert, A. Rutgersson, H. Pettersson, J.-R. Bidlot, P. A. E. M. Janssen & J. A. Polton, 2012: A global perspective on mixing in the ocean surface boundary layer. *Ocean Sciences Meeting*, Salt Lake City, UT.

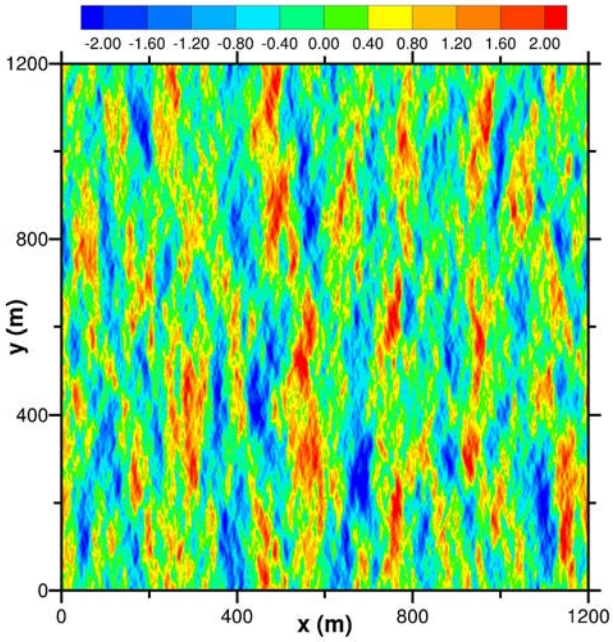

Figure 1: *A snapshot of the instantaneous wave field height $h(x, y, t)$ that is imposed at the bottom of the LES code. h is built from a sum of linear plane waves, and waves propagate in time from left to right according to the linear dispersion relationship. The horizontal grid spacing matches the LES, i.e., $\triangle x = \triangle y = 2.34$ m. The color bar is in units of meters.*

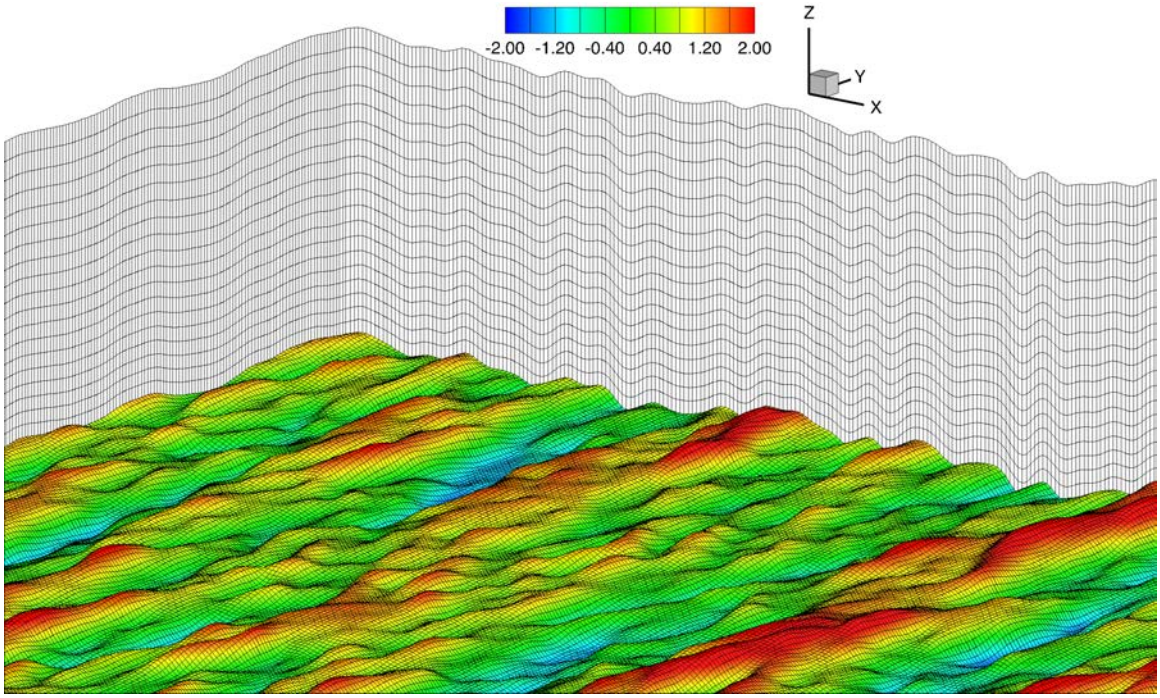

Figure 2: *An oblique 3D cutout view of the surface following computational grid used in the LES focusing on the surface layer. The extent of the vertical grid shown in the x-z and y-z planes is approximately 30 meters. Note the horizontal gridlines become level surfaces for $z>$ 100 m. The surface mesh is overlayed with color contours of wave height $h(x, y)$ in meters.*

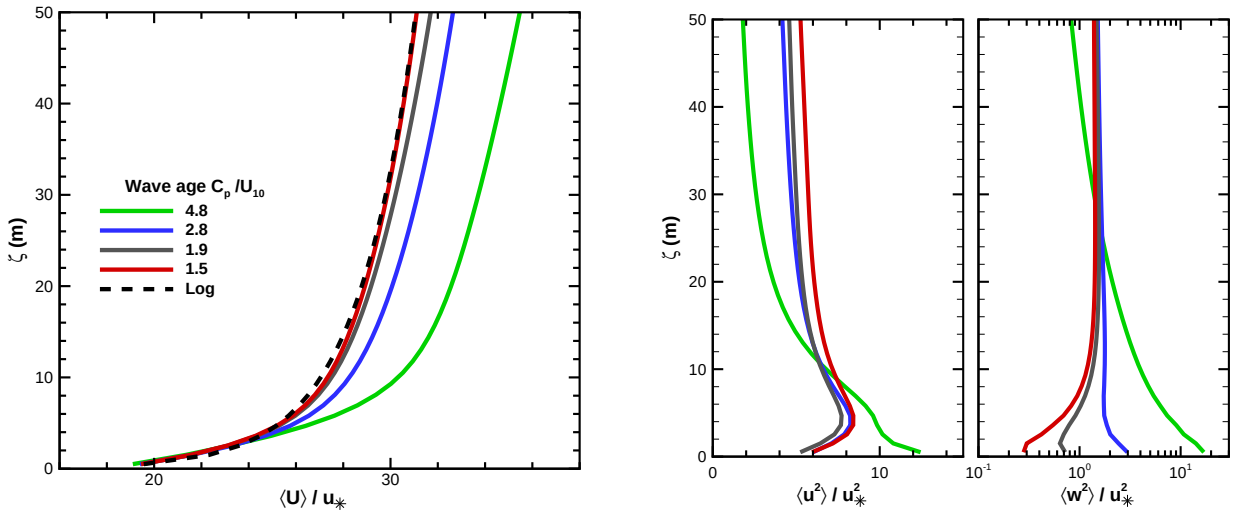

Figure 3: *Vertical profiles of wind speed (left panel) and turbulence variances (right panels) for different values of wave age $\mathcal{A} = C_p/U_{10}$. Friction velocity u_* is used for normalization. The dashed black line is the rough wall formula $U/u_* = \ln(z/z_o)/\kappa$, where $\kappa = 0.4$. Temporal and spatial averaging is used to make the statistics. The spatial averaging is over horizontal planes in computational space, i.e., at constant ζ.*

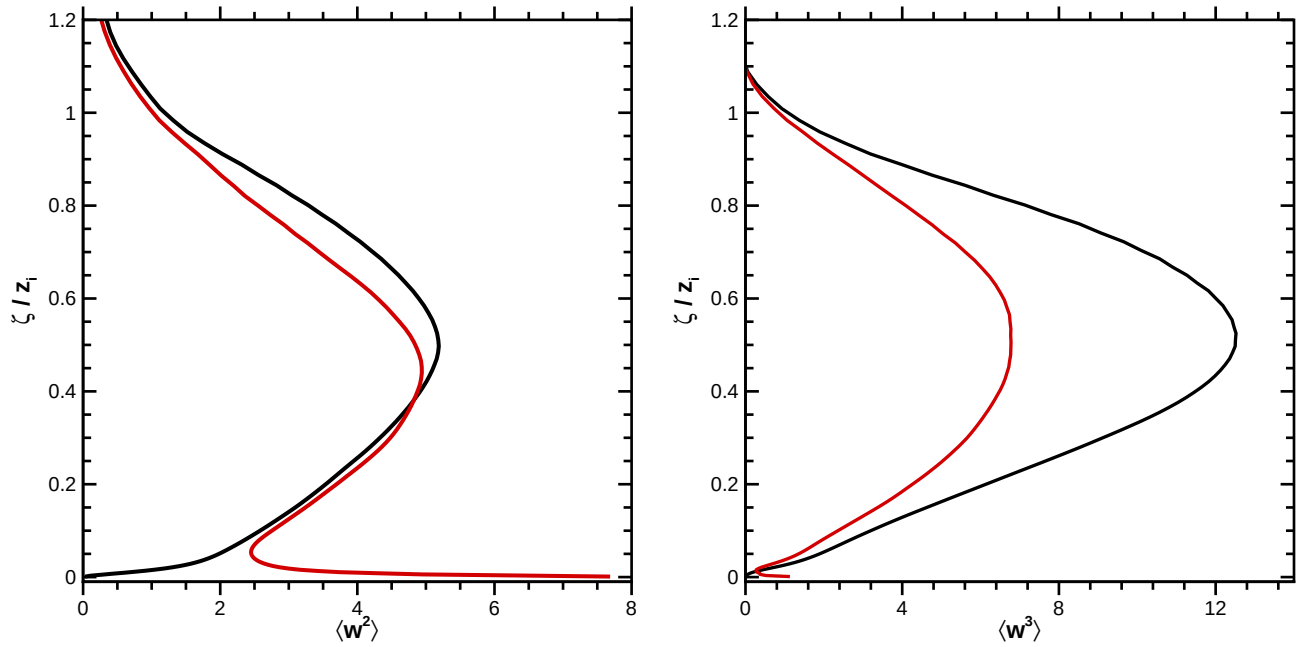

Figure 4: *Vertical profiles of vertical velocity moments $\langle \overline{w}^2 \rangle / u_*^2$ (left panel) and $\langle \overline{w}^3 \rangle / u_*^3$ (right panel) for simulations over fast moving swell (red lines) and a smooth surface (black lines). The vertical coordinate ζ is made dimensionless by the boundary layer height z_i. Note the increased velocity variance induced by moving surface waves. The smaller value of the third order moment is evidence that surface waves have modified the vertical transport of turbulent kinetic energy in this sheared-convective boundary layer.*

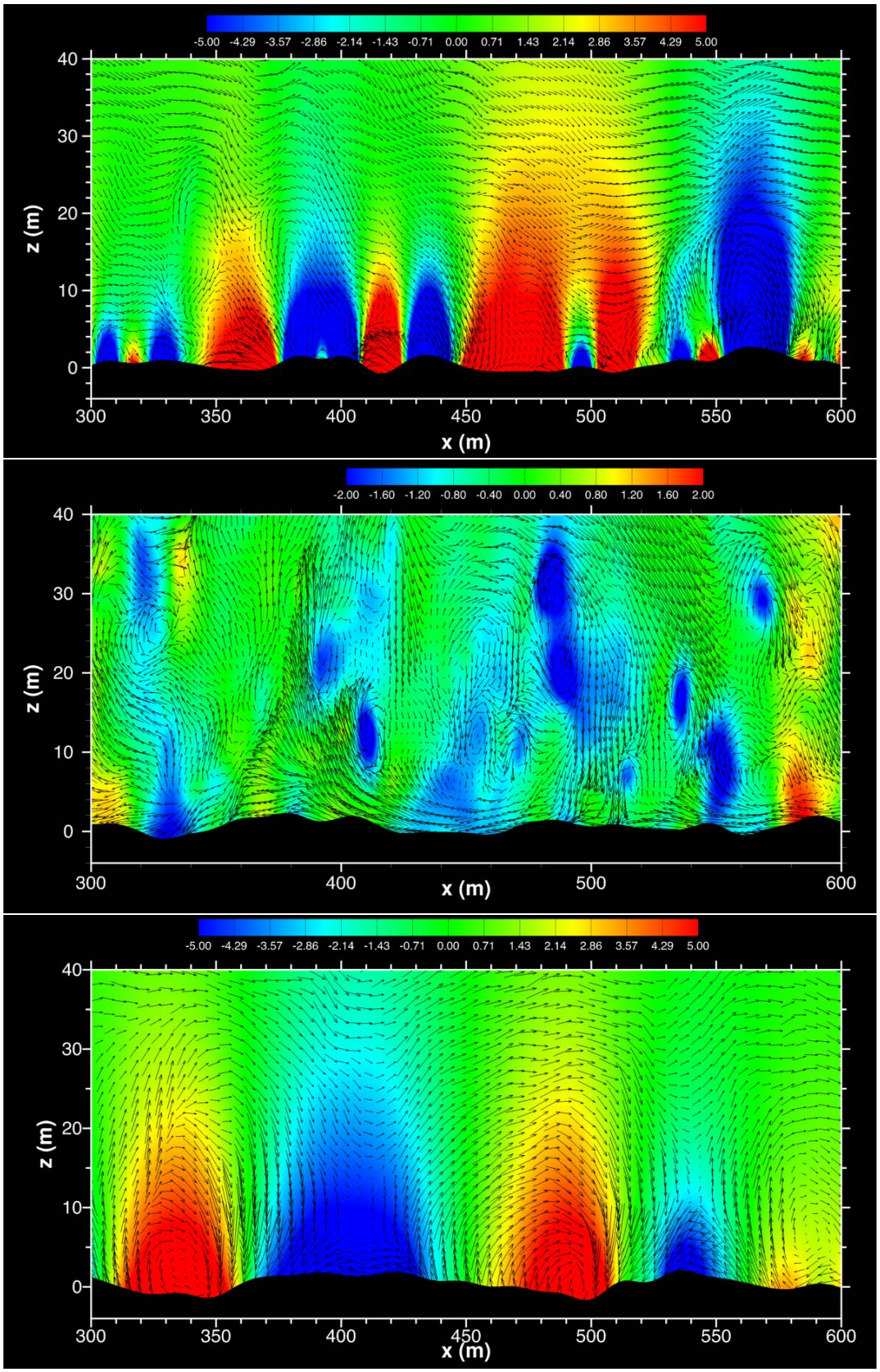

Figure 5: Vertical x-z slices of pressure fluctuation contours $\overline{p}'/\rho$ and velocity vectors ($\overline{u}$ - u_c, $\overline{w}$) in the surface layer for turbulent flow over stationary and moving waves: stationary bumps (upper panel); wind-wave equilibrium $\mathcal{A} \sim 1.5$ (middle panel); and low-wind swell dominated with $\mathcal{A} \sim 4.8$ (lower panel). The constant velocity u_c is chosen to expose the rotational motions in the surface layer.

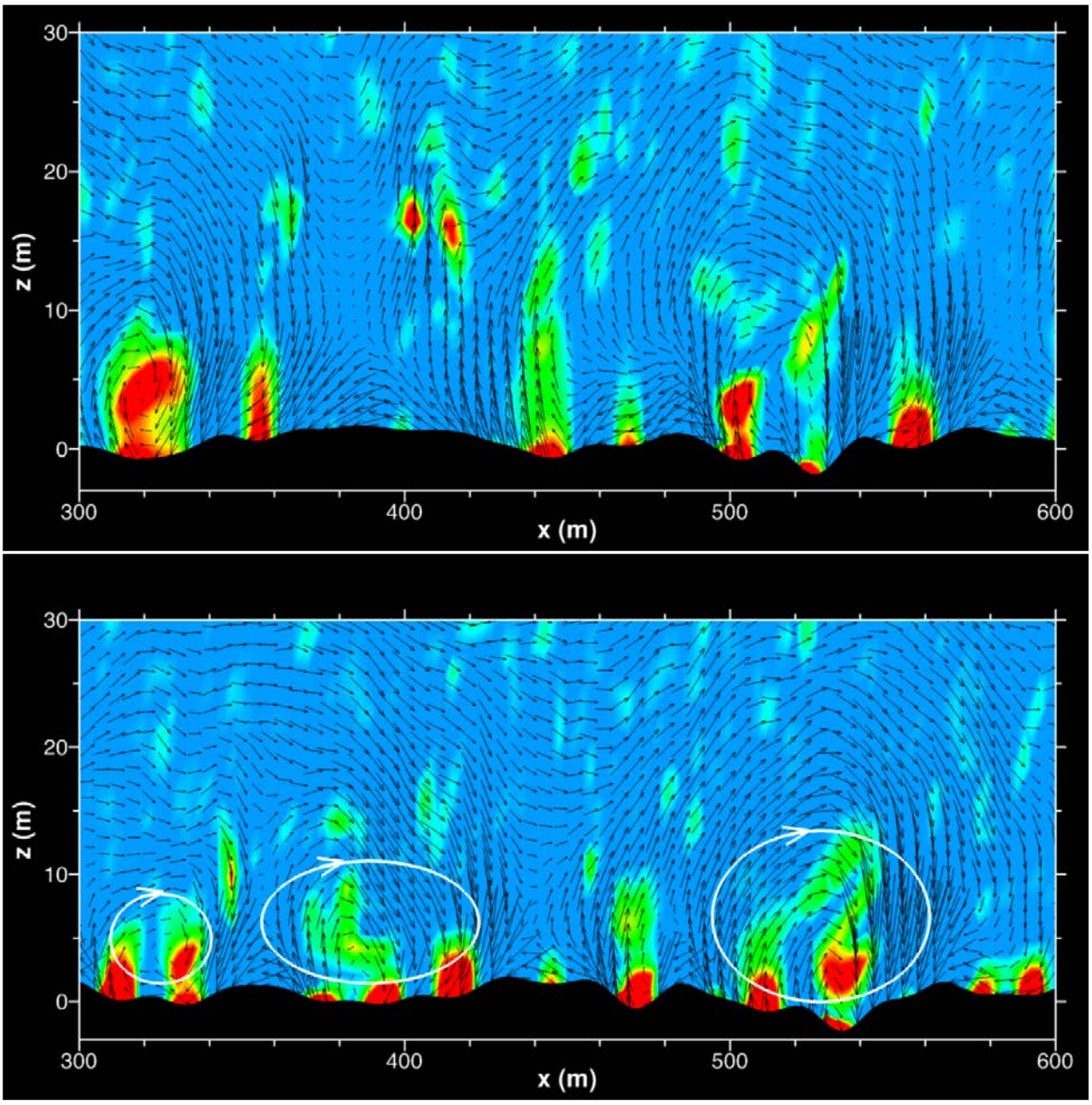

Figure 6: Contours of λ_{ci} and flow vectors ($\overline{u}$ - u_c, $\overline{w}$) in the marine surface layer for a low wind swell dominated situation with wave age $\mathcal{A} \sim 4.8$. The dark red contours of λ_{ci} are regions of strong swirling motion (vortices). Notice that the vortical motions are generally strongest in the wave troughs, and the flow vectors show that the vortical motion is clockwise. The constant velocity u_c is chosen to expose the rotational motions in the surface layer.